



Fermilab

TM-980
8050.000

BEAM TRANSPORT FOR
PRODUCING
PROTON-ANTIPROTON COLLIDING BEAMS

Mohammad Mohammadi
University of Wisconsin

Judith Nicholls
Fermilab

August 1980

This report gives an overall description of the beam transport system for the proton-antiproton colliding beam project. The original work on extraction and antiproton collection was done by George Chadwick¹ and the project was continued by Terry Rhodes². This work was modified in various ways such as to reduce β 's on the target, use existing magnets wherever possible, and introduce the lithium lenses and pulsing C magnet.

The objectives of the project are: a) to extract high energy protons (80-100 GeV/c) from the main ring and focus them onto a production target to produce antiprotons; b) to collect antiprotons and transport them to the existing booster so they can be decelerated and stacked in the cooling ring (this is repeated until enough antiprotons are collected); and c) to inject antiprotons into the main ring from the booster in the opposite direction of the proton acceleration. Notice that the reverse injection (from booster to main ring) and the antiproton production (from main ring to booster) will be done in the same channel.

The cylindrically symmetric lithium lens to be used to focus protons on the target and collect antiprotons after the target, and the very high field pulsed C magnet to be used

to separate the protons and antiprotons after the target, and their pulsers, are contributed by the Institute for Nuclear Physics, Novosibirsk, U. S. S. R.

These lines have been designed using many components salvaged from decommissioned Fermilab or Argonne beam lines. The EPB magnets are the former left bends to the Meson Hall, the 3Q120's are also from an extracted beam line, rewound with water cooled conductor for higher fields. The 5Q36's and 10IV36 are from Argonne as well as all the power supplies for the magnets.

A booster length precooling ring has been designed to collect and stochastically momentum cool antiprotons, but the beam transport for this ring is not considered in this report.

We will describe the system in three parts: a) extracted proton beam; b) antiproton collection; and c) reverse injected antiproton beam.

The extracted proton beam transport layout is shown in Figure 1. Detail of antiproton hall and the target vault are shown in Figure 2. Figure 3 is a general layout from the main ring tunnel to the booster wall.

Extracted Proton Beam

Protons at 100 GeV/c are extracted in booster length batches at a 13 Hz rate. Extraction takes place in the straight section at F-17, in the vertical direction.

At the point of extraction, the parameters of the beam are the following:

$$\begin{aligned}
 \beta_x &= 99.74754 \text{ m} & \eta_x &= 5.6474 \text{ m} \\
 \beta_y &= 30.24541 \text{ m} & \eta_x^* &= -0.099954 \\
 \alpha_x &= 1.93881 & \eta_y &= 0 \text{ m} \\
 \alpha_y &= -0.62600 & \eta_y^* &= 0 \\
 \epsilon_x &= \epsilon_y = 0.15 \pi \text{ mm mrad} \\
 \Delta p/p &= 0.082\%
 \end{aligned}$$

Some parameters for the beam line (from main ring to target) are listed below. Note that all magnet lengths are the effective lengths. The column labeled s is the length along the beam at the beginning of the element in inches (approximate). Bends are looking in the direction of the beam. Magnetic fields are in Tesla (T).

s(in)	element	length(in)	Extraction point, main ring F-17			
0.	drift	108.				
108.	Septum	204.	1.356 T	1.207 ⁰		Bend up
	(Lambertson)					
312.	drift	544.				
856.	H1 (EPB)	120.	1.590 T	0.833 ⁰		Bend right
976.	drift	12.				
988.	V1 (EPB)	120.	1.152 T	0.6035 ⁰		Bend down
1108.	drift	12.				
1120.	V2 (EPB)	120.	1.152 T	0.6035 ⁰		Bend down
1240.	drift	12.				
1252.	H2 (EPB)	120.	1.590 T	0.833 ⁰		Bend right
1372.	drift	12.				
1384.	Q1 (3Q120)	120.	-6.34 T/m			
1504.	drift	142.				
1646.	H3 (EPB)	120.	1.590 T	0.833 ⁰		Bend right
1766.	drift	300.				
2066.	Q2 (3Q120)	120.	6.34 T/m			
2186.	drift	180.				
2366.	H4 (EPB)	120.	1.590 T	0.833 ⁰		Bend right
2486.	drift	400.				
2886.	H5 (EPB)	120.	1.590 T	0.833 ⁰		Bend right
3006.	drift	400.				
3406.	H6 (EPB)	120.	1.590 T	0.833 ⁰		Bend right
3526.	drift	268.				
3794.	Q3 (3Q120)	120.	-6.34 T/m			
3914.	drift	12.				
3926.	H7 (EPB)	120.	1.590 T	0.833 ⁰		Bend right
4046.	drift	140.				
4186.	Q4 (3Q120)	120.	+4.85 T/m			
4306.	drift	140.				
4446.	H8 (EPB)	120.	1.590 T	0.833 ⁰		Bend right
4566.	drift	407.				
4973.	H9 (EPB)	120.	1.590 T	0.833 ⁰		Bend right
5093.	drift	406.				
5499.	H10 (EPB)	120.	1.590 T	0.833 ⁰		Bend right
5619.	drift	265.				
5884.	H11 (EPB)	120.	1.590 T	0.833 ⁰		Bend right
6004.	drift	78.				
6082.	Q5 (3Q120)	120.	-4.85 T/m			
6202.	drift	12.				
6214.	H12 (EPB)	120.	1.590 T	0.833 ⁰		Bend right
6334.	drift	12.				
6346.	H13 (EPB)	120.	1.590 T	0.833 ⁰		Bend right
6466.	drift	120.				
6586.	Q6 (3Q120)	120.	+4.85 T/m			
6706.	drift	687.				
7393.	H14 (EPB)	120.	1.590 T	0.833 ⁰		Bend left
7513.	drift	12.				
7525.	H15 (EPB)	120.	1.590 T	0.833 ⁰		Bend left
7645.	drift	12.				

7657.	H16 (EPB)	120.	1.590 T	0.833°	Bend left
7777.	drift	12.			
7789.	H17 (EPB)	120.	1.590 T	0.833°	Bend left
7909.	drift	12.			
7921.	H18 (EPB)	120.	1.590 T	0.833°	Bend left
8041.	drift	1072.	(includes 10" pipe)		
9113.	Q7A (3Q120)	120.	+19. T/m		
9233.	drift	15.85			
9248.8	Q7B (5Q36)	37.5	+18.5 T/m		
			(physical length = 45.2 in)		
9286.3	drift	621.65			
9908.	Q8 (3Q120)	120.	-19. T/m		
11028.	drift	54.			
10082.	Q9A (3Q120)	120.	+12.92 T/m		
10202.	drift	12.			
10214.	Q9B (3Q120)	120.	+17.44 T/m		
10334.	drift	54.			
10388.	Q10 (3Q120)	120.	-19. T/m		
10508.	drift	180.			
10788.	Center of the target				

The proton beam parameters at the center of the target (including second order effects) are the following:

$$\begin{aligned}
 \beta_x &= 11.6 \text{ cm} & \eta_x &= 0.0 \text{ } (-5 \times 10^{-6}) \text{ m} \\
 \beta_y &= 9.7 \text{ cm} & \eta_x' &= 0.0 \text{ } (+9 \times 10^{-6}) \\
 \alpha_x &= -0.081 & \eta_y &= -0.0218 \text{ m} \\
 \alpha_y &= 0.382 & \eta_y' &= 0.3419 \\
 \epsilon_x &= 0.156 \pi \text{ mm-mrad} \\
 \epsilon_y &= 0.168 \pi \text{ mm-mrad}
 \end{aligned}$$

Second order effects turned out to be minimal. The significant elements of the second order transform matrix are shown in Table I. Figures 4 and 5 are graphs of β and η as functions of s , the distance along the beam direction.

The incident beam spot size at the target is (Transport notation) $x = 0.134 \text{ mm}$, $y = 0.120 \text{ mm}$ and $x' = 1.170 \text{ mrad}$, $y' = 1.408 \text{ mrad}$.

Introducing the lithium lens in the line will reduce the spot size and β 's at this point, hence increase the capture of antiprotons. This study is the subject of another report.

Antiproton Collection

This analysis was done for collecting 6.05 GeV/c antiprotons. This transport was run in reverse -- from the booster to the target-- in order to match to the booster. The resulting parameters of the antiproton beam at production (center of the target) are:

$\beta_x = 2 \text{ cm}$
 $\beta_y = 2 \text{ cm}$ (lower β 's are conceivable)
 $\alpha_x = \alpha_y = 0.0$
 $\epsilon_x = 2.5 \pi \text{ mm-mrad}$
 $\epsilon_y = 2.0 \pi \text{ mm-mrad}$
 $\eta_{xx} = 0.0 \text{ m}$ $\eta'_x = 0.0$
 $\eta_y = 0.020 \text{ m}$ $\eta'_y = 0.015$

The first element of the line is a 5 Tesla pulsing magnet (CMAG) positioned about 13.7 inches from the center of the target. The produced antiprotons are bent upwards a total of 1.136 degrees by this magnet. They will rise by 7.3775 inches -- the difference in level between the main ring and the booster tunnel -- and will then be pitched level by another dipole (V4). The antiprotons are collected by a quadrupole triplet immediately following CMAG. This triplet is positioned on the antiproton beam axis. The surviving protons also go through this triplet, even though they have been separated from the antiprotons by CMAG, and can be dumped as soon as they exit the triplet. Notice that since the center of the two beams exiting the last quadrupole will be about 3.5 inches apart, the vacuum pipes of the quadrupoles could be as large as possible and the same shape as the quadrupole gaps.

Use of a lithium lens will definately increase the collection of antiprotons.

The antiproton collection beam line (from target to booster) is listed below.

s(in)	element	length(in)				
	Center of target					
0.	drift	13.7				
13.7	CMAG	3.15	5. T	1.136°	Bend up	
	(pulsing magnet)					
16.8	drift	4.24				
21.1	Q11 (5Q36)	37.5	-18.62 T/m			
			(physical length = 45.2 in)			
58.6	drift	30.5				
89.1	Q12 (5Q36)	37.5	+18.62 T/m			
126.6	drift	24.65				
151.2	Q13 (5Q36)	37.5	-11.38 T/m			
188.7	drift	180.75				
369.5	V4 (10IV36)	36.	.437 T	1.136°	Bend down	
405.5	drift	475.45				

881.	Q14 (5Q36)	37.5	-4.04 T/m		
918.4	drift	480.			
1398.4	Q15 (5Q36)	37.5	+1.15 T/m		
1436.	drift	1260.			
2696.	Q16 (4Q36)	36.	-0.49 T/m		
2731.	drift	1260.		(FODO starts)	
3992.	QF (4Q36)	36.	0.74 T/m		
4028.	drift	1260.			
5288.	QD (4Q36)	36.	-0.74 T/m		
5324.	drift	1260.			
6584.	QF (4Q36)	36.	+0.74 T/m		
6620.	drift	1260.			
7880.	QD (4Q36)	36.	-0.74 T/m		
7916.	drift	1260.			
9176.	QF (4Q36)	36.	+0.74 T/m		
9212.	drift	1260.			
10472.	QD (4Q36)	36.	-0.74 T/m		
10508.	drift	1260.			
11768.	QF (4Q36)	36.	+0.74 T/m		
11804.	drift	1260.			
13064.	QD (4Q36)	36.	-0.74 T/m		
13100.	drift	1260.		(FODO ends)	
14360.	drift	244.27			
14604.2	Q25 (4Q36)	36.	+3.33 T/m		
14640.2	drift	192.			
14832.2	Q26 (4Q36)	36.	-2.50 T/m		
14868.2	drift	25.64		(10.9° Bend starts)	
14894.	bend (9IV36)	36.	.700 T	1.819°	Bend right
14929.8	drift	27.28			
14957.	bend (9IV36)	36.	.700 T	1.819°	Bend right
14993.	drift	27.28			
15020.4	bend (9IV36)	36.	.700 T	1.819°	Bend right
15056.4	drift	27.28			
15083.7	bend (9IV36)	36.	.700 T	1.819°	Bend right
15119.7	drift	27.28			
15147.	bend (9IV36)	36.	.700 T	1.819°	Bend right
15183.	drift	27.28			
15210.2	bend (9IV36)	36.	.700 T	1.819°	Bend right
15246.2	drift	25.64		(10.9° Bend ends)	
15271.9	Q27 (4Q36)	36.	-1.4656 T/m		
15307.9	drift	54.			
15361.9	Q28 (4Q36)	36.	+2.98 T/m		
15397.9	drift	548.			
15945.9	Q29 (4Q36)	36.	+2.98 T/m		
15981.9	drift	54.			
16035.9	Q30 (4Q36)	36.	-3.33 T/m		
16071.9	drift	575.88			
16647.8	bend	60.	.578 T	2.5°	Bend down
16707.8	drift	340.35			
17048.7	bend	60.	.578 T	2.5°	Bend up
17108.7	drift	41.77			
	Injection into booster				

At this point:

$$\begin{aligned}
 \beta_x &= 7.592 \text{ m} & \alpha_x &= 0.490 \\
 \beta_y &= 20.494 \text{ m} & \alpha_y &= 0.150 \\
 \epsilon_x &= 2.5 \pi \text{ mm-mrad} \\
 \epsilon_y &= 2.0 \pi \text{ mm-mrad} \\
 \eta_x &= 1.8414 \text{ m} & \eta_x^1 &= 0.0 \\
 \eta_y &= 0.0 \text{ m} & \eta_y^1 &= 0.0
 \end{aligned}$$

Figures 6 and 7 are graphs of β and η .

Reverse Injected Antiproton Beam

At this stage, the booster contains antiprotons (or protons) rotating counter clockwise. Extraction is done through the same beam transport line as for injection of antiprotons, except the line is tuned for 10.9 GeV/c momentum.

The antiproton beam parameters are:

$$\begin{aligned}
 \beta_x &= 7.594 \text{ m} & \alpha_x &= 0.490 \\
 \beta_y &= 20.490 \text{ m} & \alpha_y &= 0.150 \\
 \epsilon_x &= 1.3876 \pi \text{ mm-mrad} \\
 \epsilon_y &= 1.1101 \pi \text{ mm-mrad} \\
 \eta_x &= -1.8414 \text{ m} & \eta_x^1 &= 0.0 \\
 \eta_y &= 0.0 \text{ m} & \eta_y^1 &= 0.0 \\
 \Delta p/p &= 0.1\%
 \end{aligned}$$

This beam line consists of the following:

x(in)	element	length(in)			
	Injection point in booster				
0.	drift	41.77			
41.8	bend	60.	1.041 T	2.5 °	Bend up
101.8	drift	340.35			
442.7	bend	60.	1.041 T	2.5 °	Bend down
502.7	drift	575.88			
1078.6	Q30 (4Q36)	36.	-6.00 T/m		
1114.6	drift	54.			
1168.6	Q29 (4Q36)	36.	+5.36 T/m		
1204.6	drift	548.			
1752.6	Q28 (4Q36)	36.	+5.36 T/m		
1788.6	drift	54.			
1842.6	Q27 (4Q36)	36.	-2.82 T/m		
1878.6	drift	25.64		(10.9	bend starts)
1904.2	bend (9IV36)	36.	1.262 T	1.819°	Bend left
1940.2	drift	27.28			
1967.5	bend (9IV36)	36.	1.262 T	1.819°	Bend left
2003.5	drift	27.28			

2030.8	bend (9IV36)	36.	1.262 T	1.819 ⁰	Bend left
2066.8	drift	27.28			
2094.1	bend (9IV36)	36.	1.262 T	1.819 ⁰	Bend left
2130.1	drift	27.28			
2157.4	bend (9IV36)	36.	1.262 T	1.819 ⁰	Bend left
2193.4	drift	27.28			
2220.6	bend (9IV36)	36.	1.262 T	1.819 ⁰	Bend left
2256.6	drift	25.64		(10.9 ⁰ bend ends)	
2282.3	Q26 (4Q36)	36.	-4.50 T/m		
2318.4	drift	192.			
2510.3	Q25 (4Q36)	36.	+6.00 T/m		
2546.3	drift	244.27			
2790.5	drift	1260.			(FODO starts)
4050.5	QD (4Q36)	36.	-1.61 T/m		
4086.5	drift	1260.			
5346.5	QF (4Q36)	36.	+1.61 T/m		
5382.5	drift	1260.			
6642.5	QD (4Q36)	36.	-1.61 T/m		
6678.5	drift	1260.			
7938.5	QF (4Q36)	36.	+1.61 T/m		
7974.5	drift	1260.			
9234.5	QD (4Q36)	36.	-1.61 T/m		
9270.5	drift	1260.			
10530.5	QF (4Q36)	36.	+1.61 T/m		
10566.5	drift	1260.			
11826.5	QD (4Q36)	36.	-1.61 T/m		
11862.5	drift	1260.			
13122.5	QF (4Q36)	36.	+1.61 T/m		
13158.5	drift	1260.			(FODO ends)
14418.5	Q16 (4Q36)	36.	-1.40 T/m		
14454.5	drift	1260.			
15714.5	Q15 (5Q36)	37.5	+2.66 T/m		
15752.	drift	480.			
16232.	Q14 (5Q36)	37.5	-2.29 T/m		
16269.5	drift	475.45			
16745.	V4 (10IV36)	36.	.553 T	0.797 ⁰	Bend down
			(Physical length = 51 in)		
16781.	drift	494.1			
17275.1	V3 (10IV36)	36.	.553 T	0.797 ⁰	Bend up
17311.1	drift	193.5			
17504.6	Q9B (3Q120)	120.	+1.86 T/m		
17624.6	drift	12.			
17636.6	Q9A (3Q120)	120.	-3.68 T/m		
17756.6	drift	54.			
17810.6	Q8 (3Q120)	120.	+1.67 T/m		
17930.6	drift	621.65			
18552.2	Q7B (5Q36?)	37.5	-2.89 T/m		
			(Physical length = 45.2)		
18589.7	drift	135.85			Main ring penetration

At this point (main ring penetration) the reverse beam orbit is matched to that of the extracted beam (see below).

18725.6 drift 1072.

The beam follows the extracted proton beam orbit exactly, except all elements are tuned to 10.9 GeV/c rather than 100 GeV/c.

This matching was done by fitting to the beam size, ellipse orientation, and η_y and η_y' . The resulting parameters at this point are (adjusted for momentum):

$$\begin{aligned}\beta_x &= 43.76 \text{ m} \\ \beta_y &= 117.73 \text{ m} \\ \alpha_x &= -1.415 \\ \alpha_y &= 1.821 \\ \epsilon_x &= 1.391 \pi \text{ mm mrad} \\ \epsilon_y &= 1.117 \pi \text{ mm mrad} \\ \eta_x &= \eta_x' = 0.0 \\ \eta_y &= -1.011 \text{ m} \quad \eta_y' = .020\end{aligned}$$

The values of β 's can be changed to within 10% to match the true measured values later by adjusting the gradients of the quadrupoles Q9A, Q9B, Q8, and Q7B.

Note that the reverse injection uses the same channel used for antiproton collection, but the pulsing magnet (CMAG), collecting triplet, and the quadrupoles Q7A and Q10 are turned off. The vertical pitching magnet V4 deflects the beam downward by 0.797 degrees instead of 1.136 degrees. This ensures that the reverse beam misses the production target (and the lithium lens). The beam is leveled by dipole V3.

The second order effects on this line seem to be minimal.

Figures 8 and 9 are graphs of β and η as a function of s .

Acknowledgements

We wish to acknowledge the contributions of Dave Carey and Eugene Colton.

References

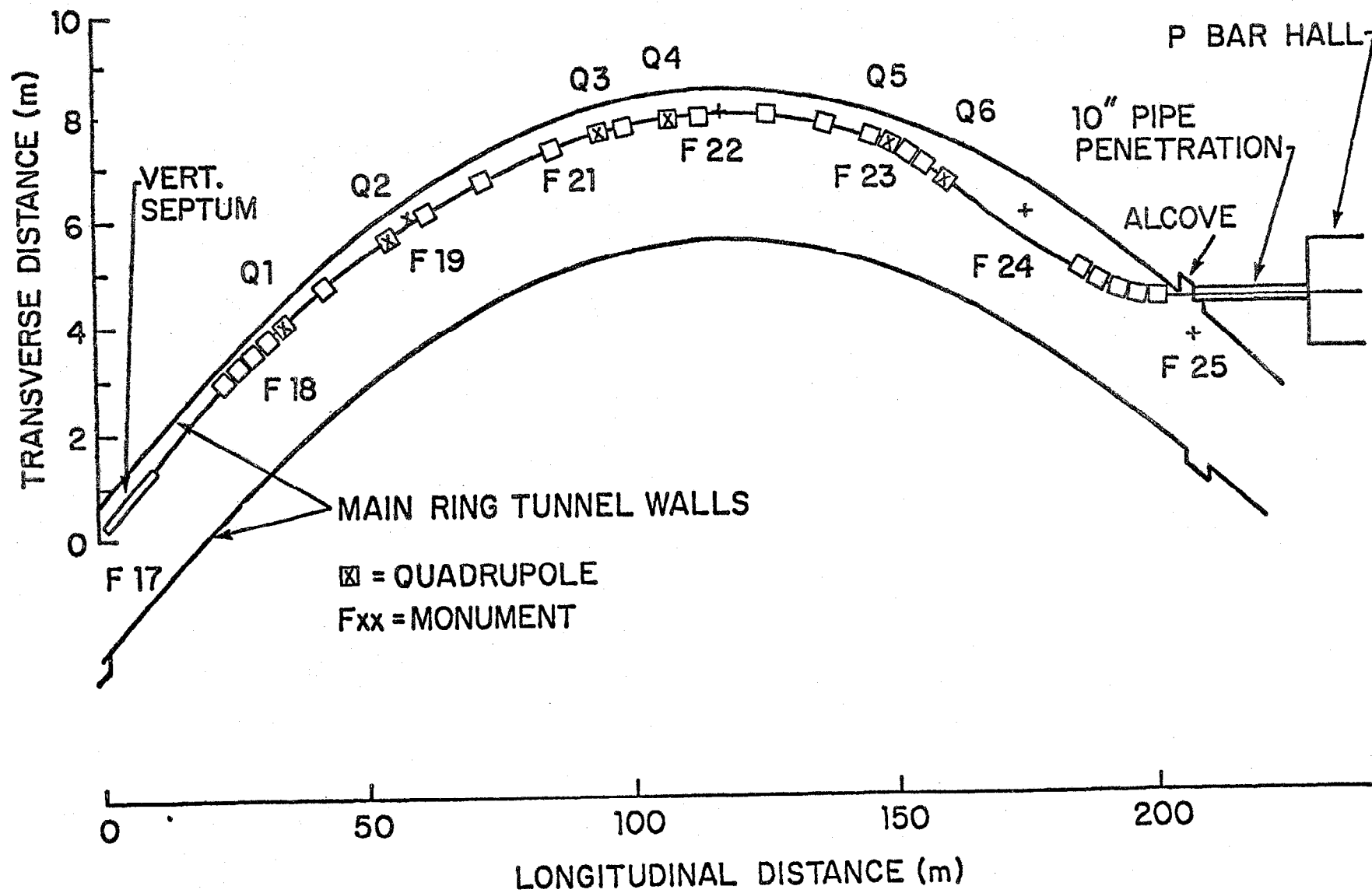
1. G. Chadwick, "Beam Transport and Target System for pp and pp Colliding Beams," Fermilab Note, Aug. 1977.
2. T. Rhodes, personal communication.
3. Don Edwards, personal communication.
4. E. L. Hubbard, "Booster Synchrotron," Fermilab TM-405.

Table I

Elements of 2nd Order Transform at the Center of the Target

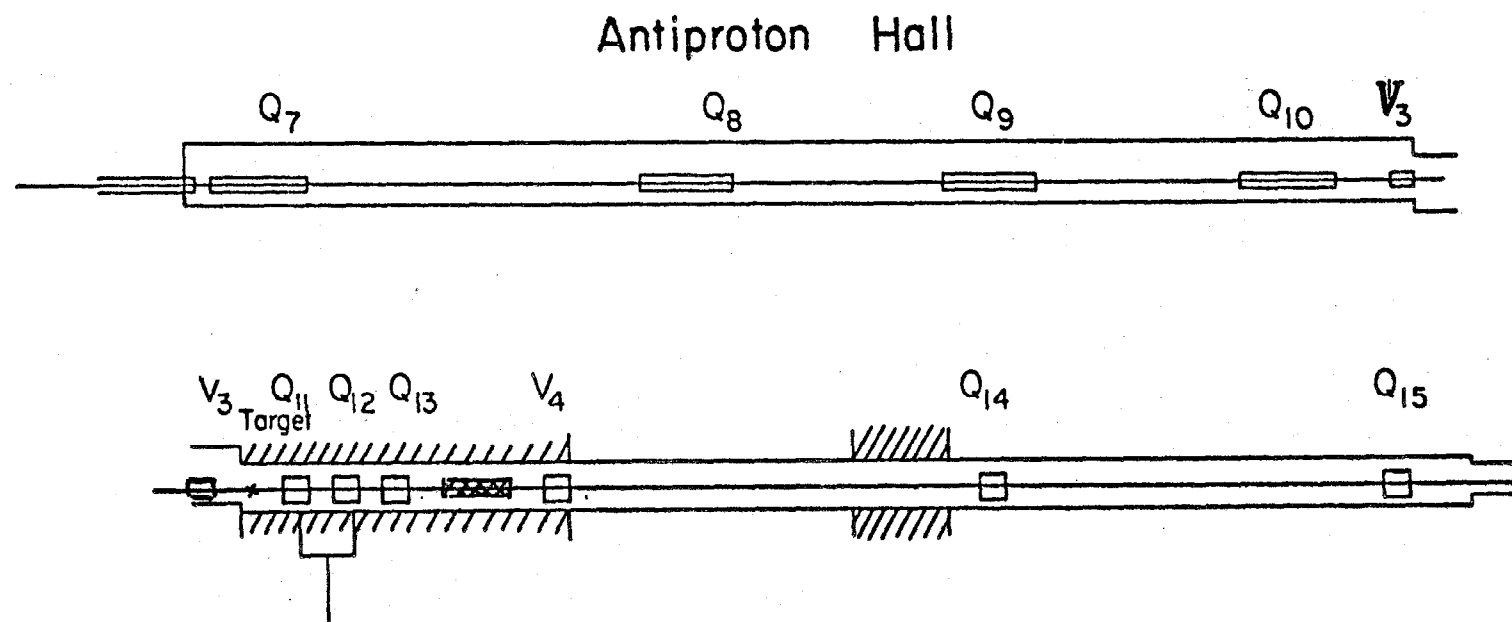
<u>Term</u>	<u>Value</u>
$T_{116} = (x x_0 \Delta p/p)$	0.264 mm/(mm-%)
$T_{126} = (x x'_0 \Delta p/p)$	9.794 mm/(mrad-%)
$T_{166} = (x \Delta p/p \Delta p/p)$	0.059 mm/mrad ²
$T_{216} = (x' x_0 \Delta p/p)$	0.017 mrad/(mm-%)
$T_{226} = (x' x'_0 \Delta p/p)$	1.046 mrad/(mrad-%)
$T_{266} = (x' \Delta p/p \Delta p/p)$	-0.081 mrad/% ²
$T_{336} = (y y_0 \Delta p/p)$	0.295 mm/(mm-%)
$T_{346} = (y y'_0 \Delta p/p)$	-6.624 mm/(mrad-%)
$T_{366} = (y \Delta p/p \Delta p/p)$	-1.419 mm/% ²
$T_{436} = (y' y_0 \Delta p/p)$	0.055 mrad/(mm-%)
$T_{446} = (y' y'_0 \Delta p/p)$	0.702 mrad/(mrad-%)
$T_{466} = (y' \Delta p/p \Delta p/p)$	-0.301 mrad/% ²
$T_{122} = (x x_0'^2)$	0.002 mm/mrad ²
$T_{222} = (x' x_0'^2)$	-0.012 mrad/mrad ²
$T_{426} = (y' x'_0 \Delta p/p)$	-0.001 mrad/(mrad-%)

All other terms are practically zero.



EXTRACTED-PROTON BEAM-TRANSPORT LAYOUT

Figure 1



\bar{p} Hall and Target Vault

Figure 2

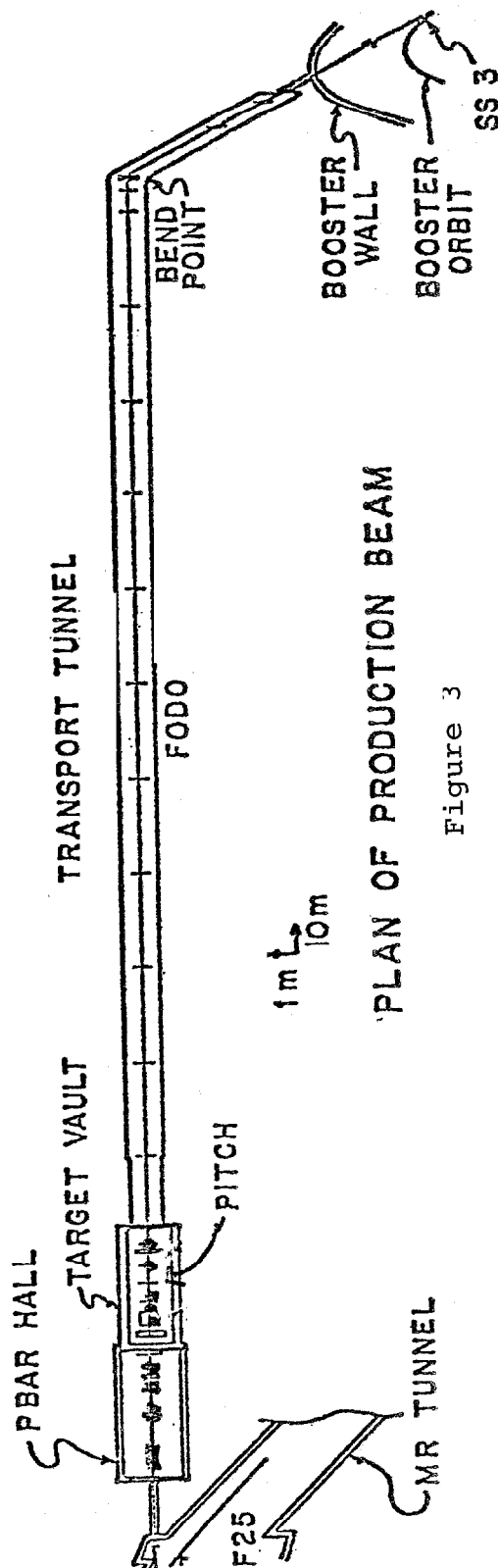
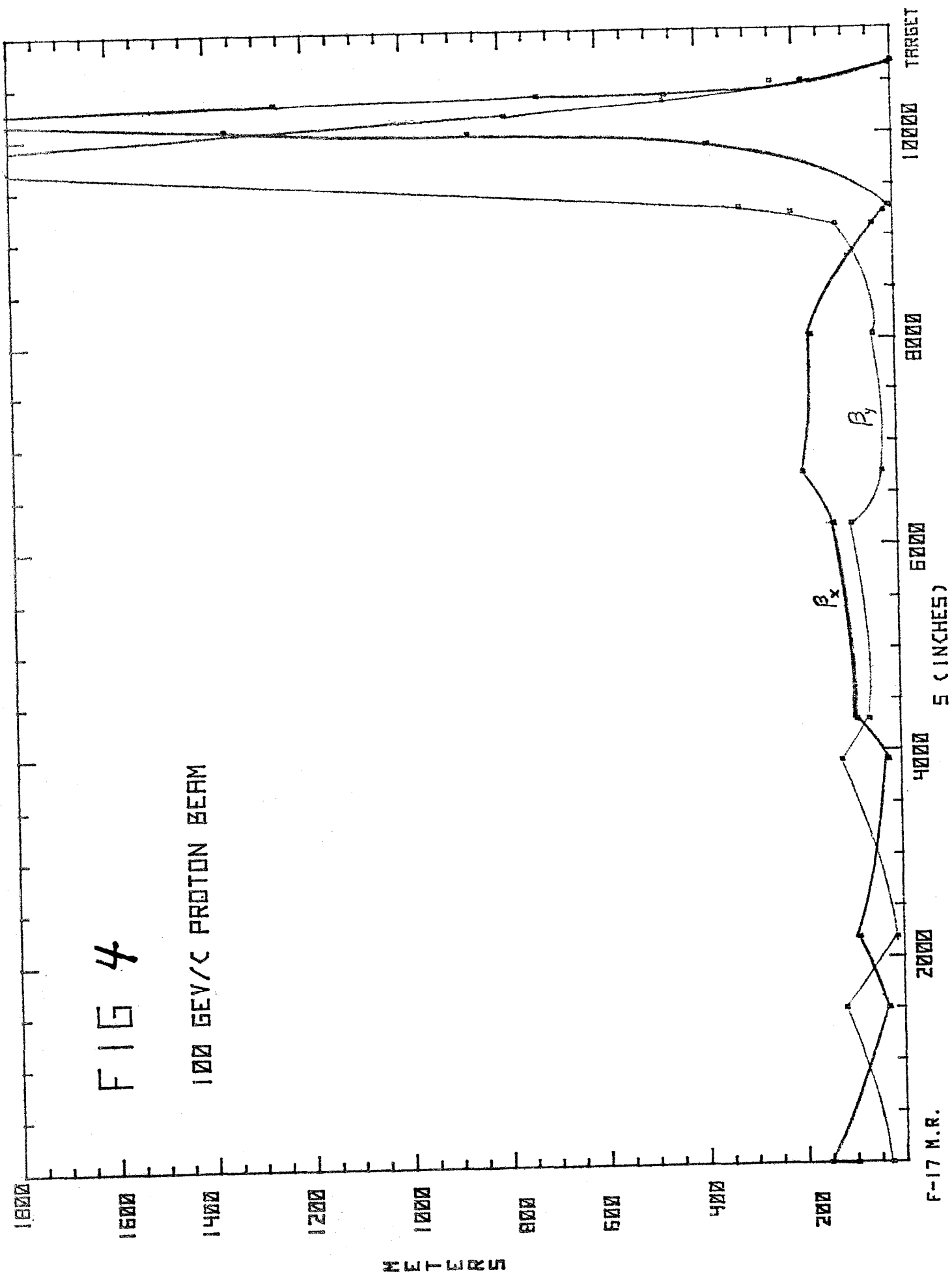


Figure 3

FIG 4

100 GEV/C PROTON BEAM



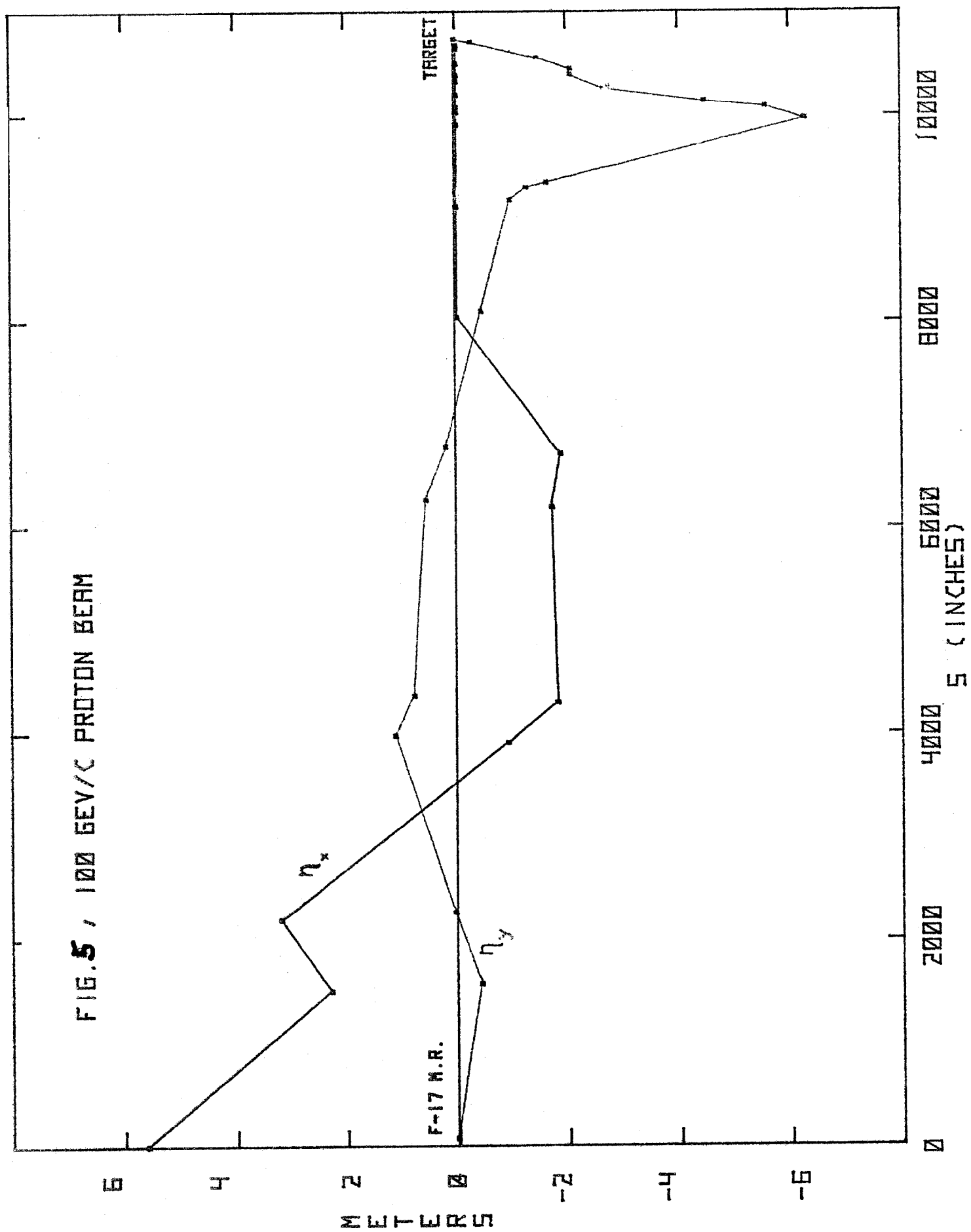


FIG. 6 REVERSE INJECTION

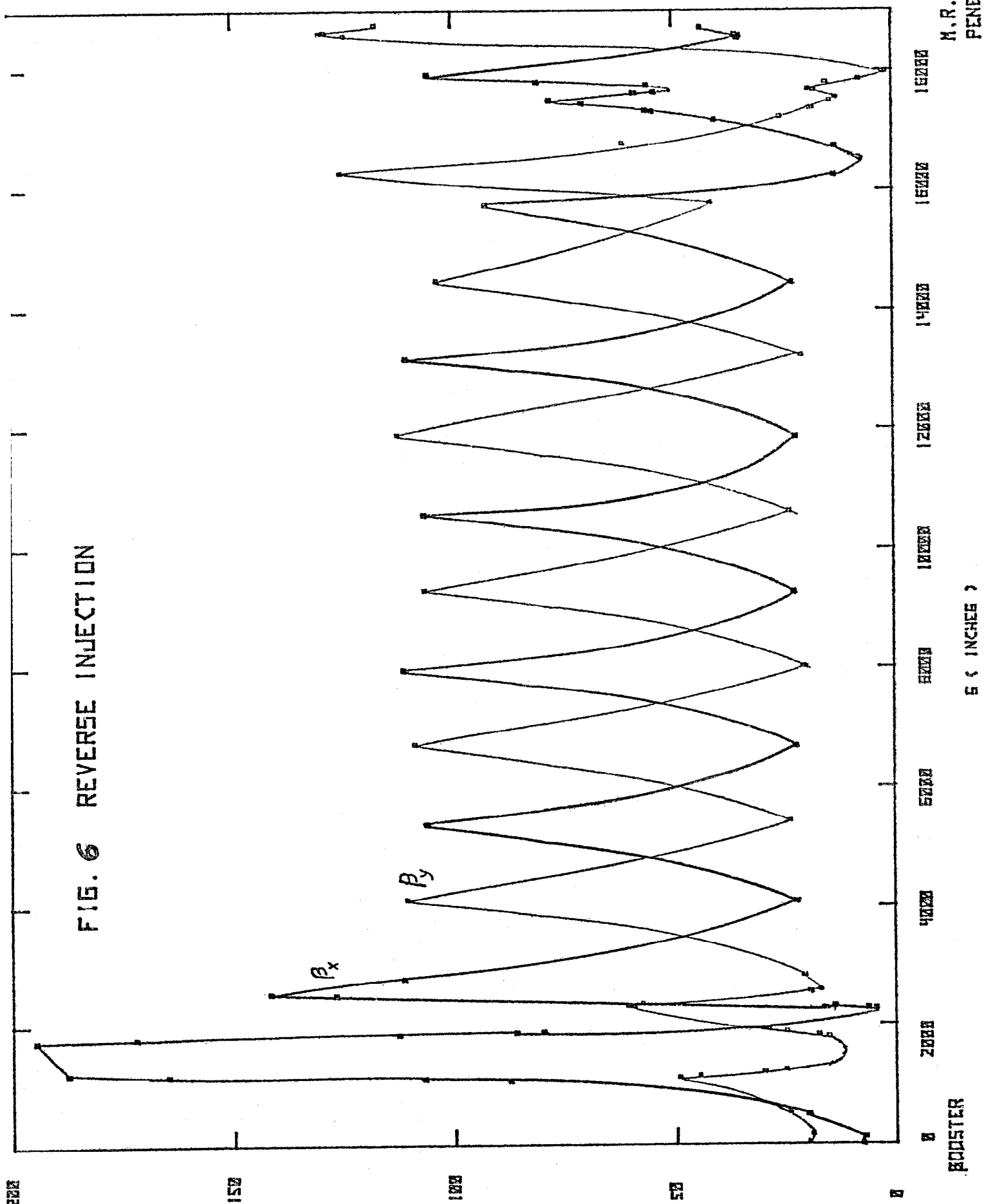


FIG. 7, REVERSE INJECTION

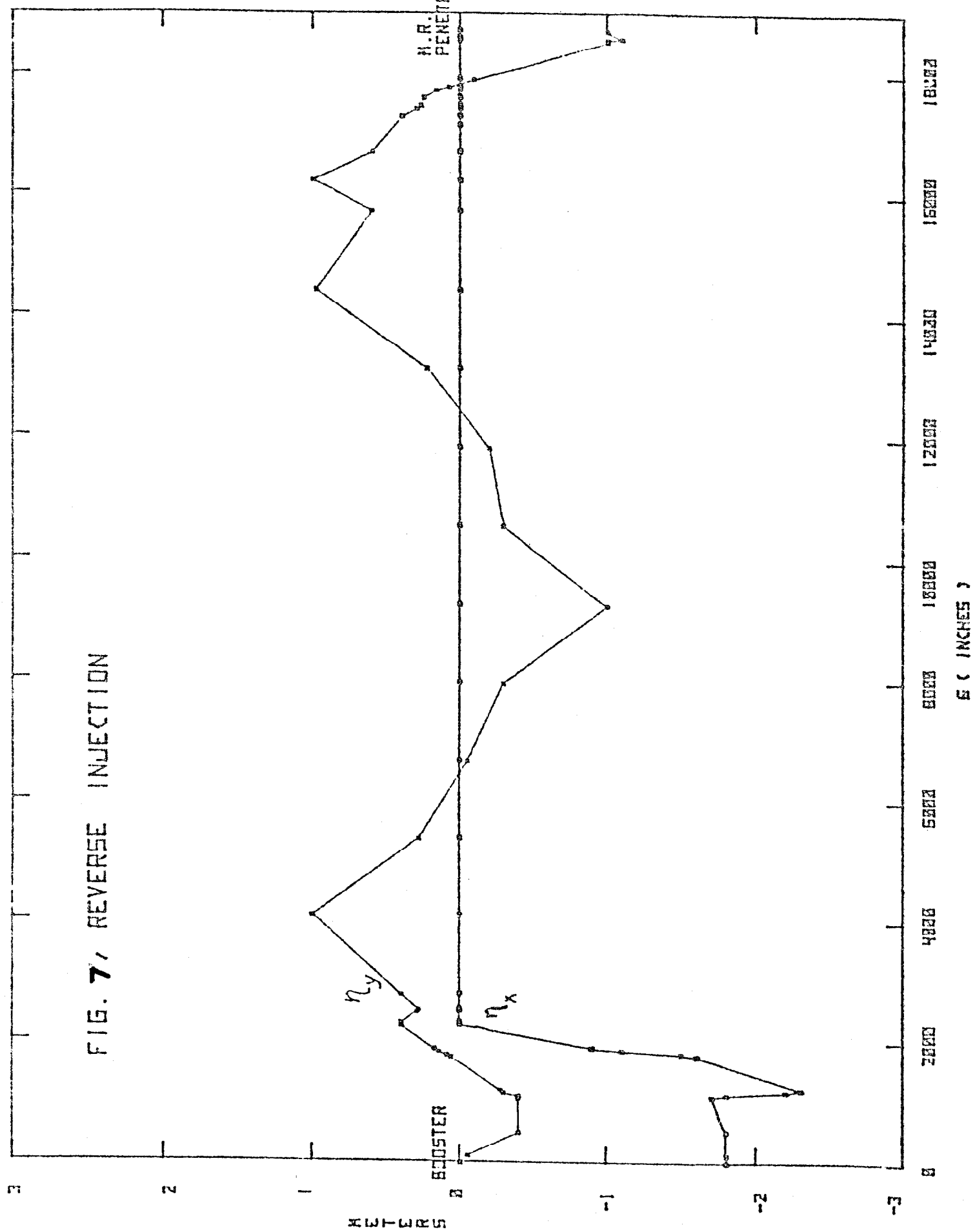


FIG. 8/ ANTI-PROTON COLLECTION

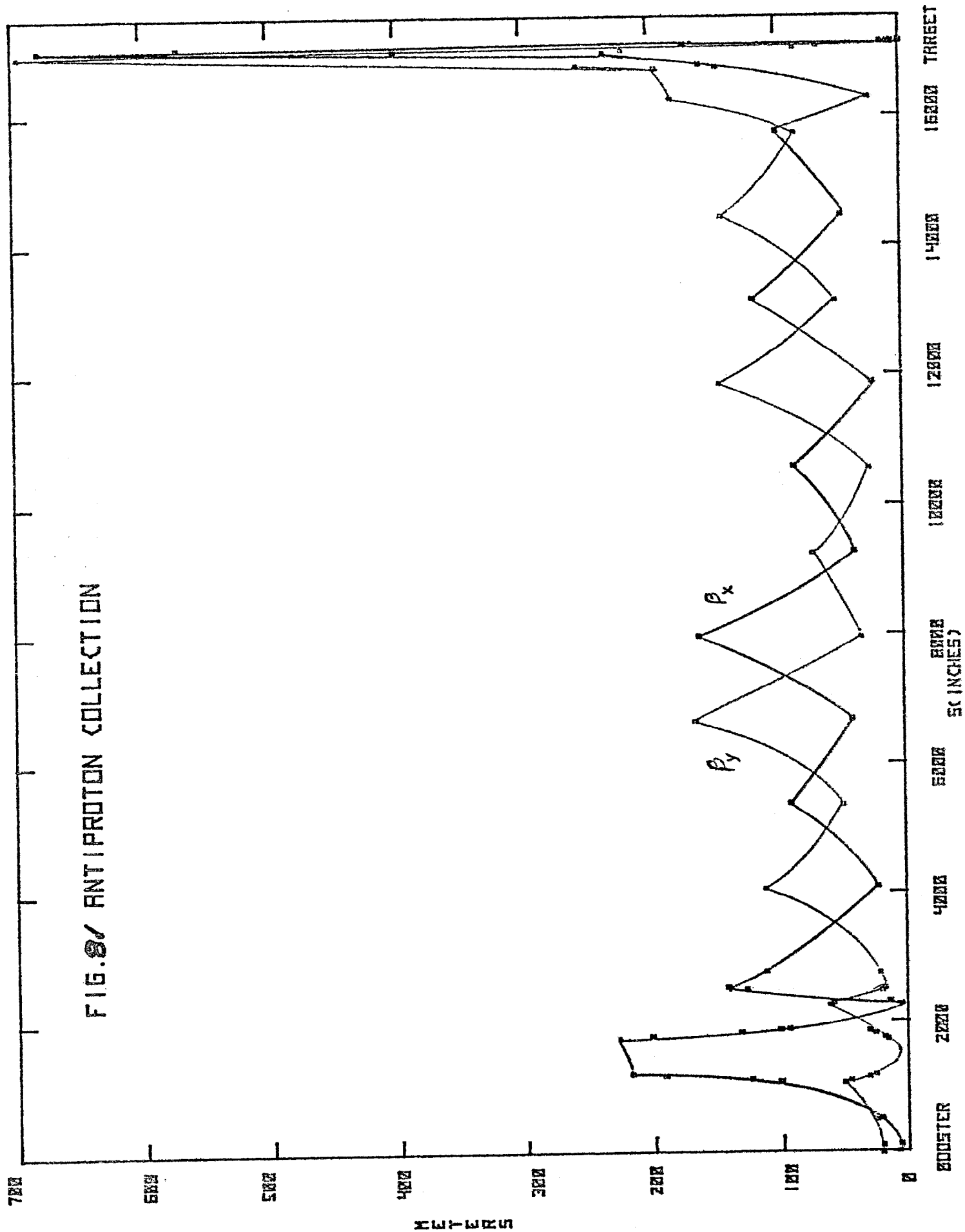


FIG. 9, ANTIPROTON COLLECTION

